JOURNAL OF Materials CHEMISTRY

# Synthesis, photophysics, photochemistry, electrochemistry and structural studies of luminescent rhenium(I) surfactant complexes; non-linear optical properties in Langmuir–Blodgett films

**Vivian Wing-Wah Yam,*[a] Victor Chor-Yue Lau,[a] Ke-Zhi Wang,[a] Kung-Kai Cheung[a] and Chun-Hui Huang[b]**

[a]*Department of Chemistry, The University of Hong Kong, Pokfulam Road, Hong Kong*
[b]*State Key Laboratory of Rare Earth Materials Chemistry and Applications, Peking University, Beijing 100871, People's Republic of China*

A series of structurally related rhenium(I) tricarbonyl diimine surfactant-active complexes, $[Re(CO)_3(diimine)\{py(CH_2)_nCH_3\}]^+$ and $[Re(CO)_3(diimine)\{pyCO(Chol)\}]^+$ have been synthesized ($n=0$, 1, 4, 12, 14, 16, 18; py = pyridyl, Chol = cholesteryl), and their photophysical, photochemical and electrochemical properties studied. A systematic study on the dependence of their photophysical properties in different environments has also been presented. In general, there is no apparent change in the photophysical behavior of these complexes as a function of the chain length of the surfactant type pyridyl ligands, the mechanism of which has been discussed. Langmuir–Blodgett films of the complexes have been prepared, and their $\pi$–$A$ isotherms, together with their electronic absorption and emission properties studied. The second harmonic generation (SHG) properties of the LB films have also been investigated. The X-ray crystal structure of a surfactant rhenium(I) complex, $[Re(bpy)(CO)_3(pyC_{17}H_{35})]ClO_4$ has been determined.

Recently, there has been a growing interest in the study of the photophysical and photochemical properties of photoactive materials in organized microheterogeneous media, in particular, surfactants.[1,2] Surfactants of amphiphilic molecules having dissimilar hydrophobic and hydrophilic regions are found to exhibit the important property of self-organization into a variety of molecular assemblies when they are exposed to environments ranging from non-polar to polar or mixed solvent systems.[1,2] Additional interests in micellar systems stem from their importance in effecting charge separation, an important process in photosynthesis.[1,2] For luminescent rhenium(I) diimine systems, the MLCT excited-state properties are very sensitive to the nature of its solvation environment, therefore by changing the environment one could easily 'tune' the excited-state properties of the complexes.[3] To our surprise, studies of the rhenium(I) diimine system in surfactant solutions have been scarce compared to its ruthenium(II) analogue, despite the fact that corresponding studies of both systems in homogeneous media are well documented.[4] With our current interests in the photophysical and photochemical studies of rhenium complexes in homogeneous solutions,[5] a program to extend our studies to microheterogeneous media was initiated. Herein are described the synthesis and photophysics of a series of new rhenium(I) surfactant complexes, $[Re(CO)_3(N{-}N)\{py(CH_2)_nCH_3\}]ClO_4$ and $[Re(CO)_3(N{-}N)\{pyCO(Chol)\}]ClO_4$ (N—N = diimine, py = pyridyl, $n=0$, 1, 4, 12, 14, 16, 18; Chol = cholesteryl). Studies on the dependence of their photophysical properties on different environments will also be described. Also, the complexes were subjected to spectroscopic and LB film deposition studies. The SHG properties of the films have also been investigated. The X-ray crystal structure of $[Re(bpy)(CO)_3(pyC_{17}H_{35})]ClO_4$ has been determined.

## Experimental

### Materials

4-Methylpyridine, 4-ethylpyridine, 2,2′-bipyridine (bpy) and 1,10-phenanthroline (phen) were obtained from Aldrich Chemical Co. The 4-substituted pyridines were distilled under reduced pressure and dried over molecular sieve before use. All the alkyl halides used in the pyridyl ligand synthesis were purchased from Aldrich Chemical Co. and used as received. Cholesterol was obtained from Lancaster and the 1,3-dicyclohexylcarbodiimide and 4-(*N*,*N*-dimethylamino)pyridine were obtained from Aldrich Chemical Co. Methyllithium in diethyl ether (1.4 M) was obtained from E. Merck and used as received. Tetrahydrofuran for ligand synthesis was distilled over sodium benzophenone under an inert atmosphere of nitrogen, and all other solvents used for syntheses were of analytical grade and were used as received. $[Re(CO)_5Cl]$ was obtained from Strem Chemicals, Inc. The complexes $[Re(L)(CO)_3(MeCN)]CF_3SO_3$ (L = bpy or phen), $[Re(bpy)(CO)_3(pyCH_3)]ClO_4$**1**, $[Re(bpy)(CO)_3(pyC_2H_5)]ClO_4$ **2** and $[Re(phen)(CO)_3(pyCH_3)]ClO_4$ **7** were prepared according to literature procedures.[6] The ligands $py(CH_2)_nCH_3$ were prepared by modification of a literature procedure.[4,7] All reactions were performed under an inert atmosphere of nitrogen.

### Synthesis of 4-pyridylcholesterolate, 4-pyCO(Chol)

The procedure was similar to that reported by Ziegler and Berger.[8] Cholesterol (1.00 g, 2.59 mmol), pyridine-4-carboxylic acid (0.32 g, 2.59 mmol), 1,3-dicyclohexylcarbodiimide (0.53 g, 2.59 mmol) and 4-(*N*,*N*-dimethylamino)pyridine (0.032 g, 0.259 mmol) were suspended in dry dichloromethane and stirred under an inert atmosphere of nitrogen for 24 h. This was followed by removal of the solvent under vacuum. The product was purified by column chromatography on silica gel with diethyl ether–light petroleum (bp 40–60 °C) (3 : 7, v/v) as eluent. The first band was unreacted cholesterol, while the second band gave the desired product, 4-pyridylcholesterolate. Yield: 1.24 g, 97%. $^1$H NMR (300 MHz, $CDCl_3$, 298 K, relative to TMS): $\delta$ 0.9–2.5 (m, 31H, cholesteric H), 4.8 (q, 1H, OCH), 5.4 (d, 1H, CH=C of cholesterol group), 7.8 (dd, 2H, pyridyl H *meta* to N), 8.7 (dd, 2H, pyridyl H *ortho* to N). IR (Nujol mull, $cm^{-1}$): $\nu$(C=O) 1800. Positive EIMS: ion clusters at $m/z$ 493 $\{M\}^+$.

### Synthesis of $[Re(CO)_3(bpy)\{py(CH_2)_nCH_3\}]ClO_4$ 1–6

The rhenium(I) complexes were prepared by modification of a literature procedure described for **1** and **2**.[6i,j] A mixture of

$[Re(bpy)(CO)_3(MeCN)]CF_3SO_3$ (100 mg, 0.16 mmol) and $py(CH_2)_nCH_3$ (0.24 mmol) in dry THF was heated to reflux under an atmosphere of nitrogen for 24 h. After cooling to room temperature, the solution was filtered and evaporated to dryness to give a bright yellow residue. This was redissolved in methanol and upon addition of $LiClO_4$, a bright yellow precipitate of the perchlorate salt was obtained. Recrystallization by vapor diffusion of diethyl ether into a dichloromethane solution of the complex gave the corresponding $[Re(bpy)(CO)_3\{py(CH_2)_nCH_3\}]ClO_4$ as air-stable bright yellow crystals. Yield: 65–88%. [**CAUTION**: perchlorate salts of metal complexes with organic ligands can be explosive and should be handled in small quantities and with great care.]

**$[Re(CO)_3(bpy)\{py(CH_2)_4CH_3\}]ClO_4$ 3.** Yield: 78%. $^1H$ NMR (300 MHz, $CDCl_3$, 298 K, relative to TMS): $\delta$ 0.85 (t, 3H, Me), 1.15–1.60 [m, 6H, $CH_2$ protons C(2)–C(4) of *n*-pentyl group], 2.55 (t, 2H, $CH_2$ attached to pyridine), 7.15 (dd, 2H, pyridyl H *meta* to N), 7.83–7.86 (2H, td, 5,5′-H of bpy), 8.00 (dd, 2H, pyridyl H *ortho* to N), 8.30–8.37 (4H, m, 3,3′ and 4,4′-H of bpy), 9.11–9.15 (2H, d, 6,6′-H of bpy). IR (Nujol mull, $cm^{-1}$): $\nu$(CO) 1917, 1932, 2028. Positive FABMS: ion clusters at *m/z* 576 $\{M\}^+$, 427 $\{M-$pentyl-py$\}^+$.

**$[Re(CO)_3(bpy)\{py(CH_2)_{14}CH_3\}]ClO_4$ 4.** Yield: 75%. $^1H$ NMR (300 MHz, $CDCl_3$, 298 K, relative to TMS): $\delta$ 0.90 (t, 3H, Me), 1.20–1.55 [m, 26H, $CH_2$ protons of C(2)–C(14) of *n*-pentadecyl group], 2.50 (t, 2H, $CH_2$ attached to pyridine), 7.10 (dd, 2H, pyridyl H *meta* to N), 7.75–7.77 (2H, td, 5,5′-H of bpy), 8.00 (dd, 2H, pyridyl H *ortho* to N), 8.30–8.37 (4H, m, 3,3′ and 4,4′-H of bpy), 9.11–9.15 (2H, d, 6,6′-H of bpy). IR (Nujol mull, $cm^{-1}$): $\nu$(CO) 1926, 1938, 2033. Positive FABMS: ion clusters at *m/z* 716 $\{M\}^+$, 427 $\{M-$pentadecyl-py$\}^+$. Elemental analyses. Found: C, 48.51; H, 5.28; N, 5.07. Calc. for $[Re(CO)_3(bpy)\{py(CH_2)_{14}CH_3\}]ClO_4$: C, 48.60; H, 5.28; N, 5.16%.

**$[Re(CO)_3(bpy)\{py(CH_2)_{16}CH_3\}]ClO_4$ 5.** Yield: 75%. $^1H$ NMR (300 MHz, $CDCl_3$, 298 K, relative to TMS): $\delta$ 0.90 (t, 3H, Me), 1.20–1.55 [m, 30H, $CH_2$ protons of C(2)–C(16) of *n*-heptadecyl group], 2.50 (t, 2H, $CH_2$ attached to pyridine), 7.10 (dd, 2H, pyridyl H *meta* to N), 7.75–7.77 (2H, td, 5,5′-H of bpy), 8.00 (dd, 2H, pyridyl H *ortho* to N), 8.30–8.37 (4H, m, 3,3′ and 4,4′-H of bpy), 9.11–9.15 (2H, d, 6,6′-H of bpy). IR (Nujol mull, $cm^{-1}$): $\nu$(CO) 1926, 1938, 2032. Positive FABMS: ion clusters at *m/z* 744 $\{M\}^+$, 427 $\{M-$heptadecyl-py$\}^+$. Elemental analyses. Found: C, 49.78; H, 5.54; N, 4.92. Calc. for $[Re(CO)_3(bpy)\{py(CH_2)_{16}CH_3\}]ClO_4$: C, 49.84; H, 5.58; N, 4.98%.

**$[Re(CO)_3(bpy)\{py(CH_2)_{18}CH_3\}]ClO_4$ 6.** Yield: 68%. $^1H$ NMR (300 MHz, $CDCl_3$, 298 K, relative to TMS): $\delta$ 0.90 (t, 3H, Me), 1.20–1.55 [m, 34H, $CH_2$ protons of C(2)–C(18) of *n*-nonadecyl group], 2.50 (t, 2H, $CH_2$ attached to pyridine), 7.15 (dd, 2H, pyridyl H *meta* to N), 7.75–7.77 (2H, td, 5,5′-H of bpy), 8.00 (dd, 2H, pyridyl H *ortho* to N), 8.30–8.37 (4H, m, 3,3′ and 4,4′-H of bpy), 9.11–9.15 (2H, d, 6,6′-H of bpy). IR (Nujol mull, $cm^{-1}$): $\nu$(CO) 1911, 1932, 2030. Positive FABMS: ion clusters at *m/z* 772 $\{M\}^+$, 427 $\{M-$nonadecyl-py$\}^+$. Elemental analyses. Found (%): C, 47.59; H, 5.17; N, 4.31. Calc. for $[Re(CO)_3(bpy)\{py(CH_2)_{18}CH_3\}]ClO_4\cdot CH_2Cl_2$: C, 47.71; H, 5.54; N, 4.39%.

### Synthesis of $[Re(CO)_3(phen)\{py(CH_2)_nCH_3\}]ClO_4$ 7–12

The complexes were prepared similarly to that described for the preparation of **1**–**6** except 1,10-phenanthroline (phen) was used instead of 2,2′-bipyridine (bpy). Yield: 75–88%.

**$[Re(CO)_3(phen)\{py(CH_2)_4CH_3\}]ClO_4$ 8.** Yield: 83%. $^1H$ NMR (300 MHz, $CDCl_3$, 298 K, relative to TMS): $\delta$ 0.85 (3H, t, Me), 1.18–1.50 [6H, m, $CH_2$ protons of C(2)–C(4) of *n*-pentyl group], 2.50 (2H, t, $CH_2$ attached to pyridine), 7.10 (2H, dd, pyridyl H *meta* to N), 8.10 (dd, 2H, pyridyl H *ortho* to N), 8.21–8.23 (4H, m, 3,8- and 5,6-H of phen), 8.83–8.86 (2H, 4,7-H of phen), 9.58–9.60 (2H, 2,9-H of phen). IR (Nujol mull, $cm^{-1}$): $\nu$(CO) 1904, 1931, 2030. Positive FABMS: ion clusters at *m/z* 600 $\{M\}^+$, 451 $\{M-$pentyl-py$\}^+$.

**$[Re(CO)_3(phen)\{py(CH_2)_{12}CH_3\}]ClO_4$ 9.** Yield: 83%. $^1H$ NMR (300 MHz, $CDCl_3$, 298 K, relative to TMS): $\delta$ 0.90 (3H, t, Me), 1.15–1.50 [22H, m, $CH_2$ protons of C(2)–C(12) of *n*-tridecyl group], 2.45 (2H, t, $CH_2$ attached to pyridine), 7.05 (2H, dd, pyridyl H *meta* to N), 8.10 (dd, 2H, pyridyl H *ortho* to N), 8.21–8.23 (4H, m, 3,8- and 5,6-H of phen), 8.83–8.86 (2H, 4,7-H of phen), 9.58–9.60 (2H, 2,9-H of phen). IR (Nujol mull, $cm^{-1}$): $\nu$(CO) 1902, 1930, 2031. Positive FABMS: ion clusters at *m/z* 712 $\{M\}^+$, 451 $\{M-$tridecyl-py$\}^+$.

**$[Re(CO)_3(phen)\{py(CH_2)_{14}CH_3\}]ClO_4$ 10.** Yield: 83%. $^1H$ NMR (300 MHz, $CDCl_3$, 298 K, relative to TMS): $\delta$ 0.90 (3H, t, Me), 1.15–1.50 [26H, m, $CH_2$ protons of C(2)–C(14) of *n*-pentadecyl group], 2.45 (2H, t, $CH_2$ attached to pyridine), 7.05 (2H, dd, pyridyl H *meta* to N), 8.10 (dd, 2H, pyridyl H *ortho* to N), 8.21–8.23 (4H, m, 3,8- and 5,6-H of phen), 8.83–8.86 (2H, 4,7-H of phen), 9.58–9.60 (2H, 2,9-H of phen). IR (Nujol mull, $cm^{-1}$): $\nu$(CO) 1901, 1928, 2032. Positive FABMS: ion clusters at *m/z* 712 $\{M\}^+$, 451 $\{M-$pentadecyl-py$\}^+$. Elemental analyses. Found: C, 50.90; H, 5.37; N, 4.89. Calc. for $[Re(CO)_3(phen)\{py(CH_2)_{14}CH_3\}]ClO_4\cdot 0.5\ Et_2O$: C, 50.57; H, 5.69; N, 4.78%.

**$[Re(CO)_3(phen)\{py(CH_2)_{16}CH_3\}]ClO_4$ 11.** Yield: 80%. $^1H$ NMR (300 MHz, $CDCl_3$, 298 K, relative to TMS): $\delta$ 0.90 (3H, t, Me), 1.15–1.50 [30H, m, $CH_2$ protons of C(2)–C(16) of *n*-heptadecyl group], 2.45 (2H, t, $CH_2$ attached to pyridine), 7.05 (2H, dd, pyridyl H *meta* to N), 8.10 (2H, dd, pyridyl H *ortho* to N), 8.21–8.23 (4H, m, 3,8- and 5,6-H of phen), 8.83–8.86 (2H, 4,7-H of phen), 9.58–9.60 (2H, 2,9-H of phen). IR (Nujol mull, $cm^{-1}$): $\nu$(CO) 1907, 1928, 2032. Positive FABMS: ion clusters at *m/z* 712 $\{M\}^+$, 451 $\{M-$heptadecyl-py$\}^+$. Elemental analyses. Found: C, 51.32; H, 5.48; N, 4.71. Calc. for $[Re(CO)_3(phen)\{py(CH_2)_{16}CH_3\}]ClO_4$: C, 51.23; H, 5.42; N, 4.85%.

**$[Re(CO)_3(phen)\{py(CH_2)_{18}CH_3\}]ClO_4$ 12.** Yield: 75%. $^1H$ NMR (300 MHz, $CDCl_3$, 298 K, relative to TMS): $\delta$ 0.90 (3H, t, Me), 1.15–1.50 [m, 34H, $CH_2$ protons of C(2)–C(18) of *n*-nonadecyl group], 2.50 (2H, t, $CH_2$ attached to pyridine), 7.10 (2H, dd, pyridyl H *meta* to N), 8.10 (dd, 2H, pyridyl H *ortho* to N), 8.21–8.23 (4H, m, 3,8- and 5,6-H of phen), 8.83–8.86 (2H, 4,7-H of phen), 9.58–9.60 (2H, 2,9-H of phen). IR (Nujol mull, $cm^{-1}$): $\nu$(CO) 1905, 1928, 2032. Positive FABMS: ion clusters at *m/z* 796 $\{M\}^+$, 451 $\{M-$nonadecyl-py$\}^+$. Elemental analyses. Found: C, 52.58; H, 5.74; N, 4.67. Calc. for $[Re(CO)_3(phen)\{py(CH_2)_{18}CH_3\}]ClO_4$: C, 52.31; H, 5.70; N, 4.69%.

### Synthesis of $[Re(CO)_3(N-N)\{4\text{-}pyCO(Chol)\}]ClO_4$ (N–N = bpy or phen)

The complexes were prepared in similar manner to the preparation of **1**–**12** except 4-pyridylcholesterolate was used instead of the surfactant pyridyl ligand.

**$[Re(CO)_3(bpy)\{4\text{-}pyCO(Chol)\}]ClO_4$ 13.** Yield: 75%. $^1H$ NMR (300 MHz, $CDCl_3$, 298 K, relative to TMS): $\delta$ 0.9–2.5 (m, 31H, cholesteric H), 4.8 (q, 1H, OCH), 5.4 (d, 1H, CH=C of cholesterol group), 7.75–7.77 (2H, td, 5,5′-H of bpy), 7.88–7.91 (dd, 2H, pyridyl H *meta* to N), 8.31–8.34 (4H, m, 3,3′-H and 4,4′-H of bpy), 8.72–8.75 (dd, 2H, pyridyl H *ortho*

to N), 9.06–9.08 (2H, 6,6′-H of bpy); IR (Nujol mull, $cm^{-1}$): $\nu$(C=O) 1800; $\nu$(CO) 1918, 1934, 2031. Positive FABMS: ion clusters at $m/z$ 919 $\{M\}^+$, 427 $\{M-4\text{-pyCO(Chol)}\}^+$. Elemental analyses. Found: C, 54.32; H, 5.65; N, 4.37. Calc. for $[Re(CO)_3(bpy)\{4\text{-pyCO(Chol)}\}]ClO_4$: C, 54.22; H, 5.70; N, 4.13%.

**$[Re(CO)_3(phen)\{4\text{-pyCO(Chol)}\}]ClO_4$ 14.** Yield: 77%. $^1H$ NMR (300 MHz, $CDCl_3$, 298 K, relative to TMS): $\delta$ 0.9–2.5 (m, 31H, cholesteric H), 4.8 (q, 1H, OCH), 5.4 (d, 1H, CH=C of cholesterol group), 7.76–7.79 (td, 2H, 5,5′-H of bpy), 7.88–7.91 (dd, 2H, pyridyl H *meta* to N), 8.31–8.37 (m, 4H, 4,4′-H of bpy and pyridyl H *ortho* to N), 8.72–8.75 (2H, d, 3,3′-H of bpy), 9.09–9.11 (2H, dd, 6,6′-H of bpy). IR (Nujol mull, $cm^{-1}$): $\nu$(C=O) 1810; $\nu$(CO) 1909, 1928, 2032. Positive FABMS: ion clusters at $m/z$: 943 $\{M\}^+$, 451 $\{M-4\text{-pyCO(Chol)}\}^+$. Elemental analyses. Found: C, 55.26; H, 5.55; N, 3.88. Calc. for $[Re(CO)_3(phen)\{4\text{-PyCO(Chol)}\}]ClO_4$: C, 55.28; H, 5.76; N, 4.03.

### Physical measurements and instrumentation

UV–VIS absorption spectra were obtained on a Hewlett Packard 8452A diode array spectrophotometer, IR spectra as Nujol mulls on a Bio-Rad FTS-7 Fourier-transform IR spectrophotometer (4000–400 $cm^{-1}$), and steady-state excitation and emission spectra on a Spex Fluorolog 111 spectrofluorometer equipped with a Hamamatsu R-928 photomultiplier tube. Low-temperature (77 K) spectra were recorded by using an optical Dewar sample holder. $^1H$ NMR spectra were recorded on a 300 MHz Bruker DPX300 Fourier-transform NMR spectrometer. Chemical shifts ($\delta$) were reported relative to tetramethylsilane (TMS). Electron-impact (EI) and positive ion FAB mass spectra were collected on a Finnigan MAT95 mass spectrometer. Elemental analyses of the new complexes were performed by the Butterworth Laboratories Ltd.

Emission-lifetime measurements were performed using a conventional laser system. The excitation source was the 355 nm output (third harmonic) of a Quanta-Ray Q-switched GCR-150–10 pulsed Nd-YAG laser. Luminescence decay signals were recorded on a Tektronix model TDS-620A (500 MHz, $2\times10^9$ samples $s^{-1}$) digital oscilloscope, and analyzed using a program for exponential fits. All solutions for photophysical studies were prepared under vacuum in a 10 $cm^3$ round-bottom flask equipped with a side-arm 1 cm fluorescence cuvette and sealed from the atmosphere by a Kontes quick-release Teflon stopper. Solutions were rigorously degassed with no fewer than four freeze–pump–thaw cycles.

Cyclic voltammetric measurements were performed by using a CH Instrument Inc., model CHI 620 Electroanalytical Analyzer, interfaced to an IBM-compatible personal computer. The ferrocenium–ferrocene couple was used as the internal standard in the electrochemical measurements in acetonitrile (0.1 M $Bu^n_4NPF_6$). The working electrode was a glassy carbon (Atomergic Chemetals V25) electrode, with a $Ag/AgNO_3$ (0.1 M in MeCN) electrode as the reference electrode and a platinum foil acting as the counter electrode.

**Sample preparation for the LB films.** Langmuir–Blodgett film deposition was performed using a Nima Technology model 622 Langmuir–Blodgett trough. The rhenium(I) complexes were first dissolved in chloroform (AR, Ajax) at a concentration of 1 mg $ml^{-1}$, and the solutions were then spreaded onto a pure water subphase (18 °C, pH 5.6). After complete evaporation of the solvent, the surface pressure–area isotherms were recorded at a barrier compression speed of 22 $cm^2$ $min^{-1}$. At a constant pressure, *i.e.* the deposition pressure which differs for different complexes (Table 5), the floating films were transferred onto the hydrophobically pretreated substrates (quartz) by the vertical dipping (VD) method with a dipping speed of 5 mm $min^{-1}$. The deposition occurred upon upstroke to give the multilayer films with Z-type structure.[9] For the emission measurements, emission spectra of the LB films were recorded in the front face mode.

**NLO measurements of the LB films.** The measurements were performed in the transmission geometry using a Y-cut quartz crystal as reference[10] and a Quanta-Ray Q-switched GCR-150–10 Nd : YAG laser with fundamental frequency of 1.064 μm as the laser source. A 1/2 $\lambda$ plate and a Glan–Taylor polarizer were used to vary the polarization direction of the laser beam. The fundamental light, linearly polarized either parallel (p) or perpendicular (s) to the plane of incidence, was focused by a quartz lens (50 mm focal length) and was directed at an incident angle of 45° onto the vertically mounted sample. Behind the film, a series of filters and a monochromator were used to ensure that only the second harmonic radiation was detected by the photomultiplier tube. The average output signal was recorded on a Tektronix TDS 620A digitized storage oscilloscope.

Prior to the SHG measurements, the films at the back side of the substrates were wiped off carefully with lens tissues soaked with chloroform in order to prevent interference from signals arising from the monolayers at the front and the backside of the substrate.

**Crystal structure determination.** Crystals of **5** were obtained by slow diffusion of diethyl ether into their dichloromethane solution.

*Crystal data for* **5**. $[C_{35}H_{47}N_3O_3Re]^+ClO_4^-$; $M=843.43$, triclinic, space group $P\bar{1}$ (no. 2), $a=11.068(3)$, $b=21.679(5)$, $c=8.694(2)$ Å, $\alpha=92.48(2)$, $\beta=112.90(2)$, $\gamma=99.93(2)°$, $V=1878.8(9)$ $Å^3$, $Z=2$, $D_c=1.491$ g $cm^{-3}$, $\mu$(Mo-K$\alpha$)=33.54 $cm^{-1}$, $F(000)=852$, $T=298$ K. A crystal of dimensions $0.15\times0.10\times0.20$ mm was used for data collection at 25 °C on a Rigaku AFC7R diffractometer with graphite monochromatized Mo-K$\alpha$ radiation ($\lambda=0.71073$ Å) using $\omega$–$2\theta$ scans with $\omega$-scan angle $(1.31+0.35\tan\theta)°$ at a scan speed of 16.0 degrees $min^{-1}$ [up to four scans for reflections with $I<15\sigma(I)$]. Intensity data (in the range of $2\theta_{max}=45°$; $h$, 0–11; $k$, −21 to 21; $l$, −8 to 8 and three standard reflections measured after every 300 reflections showed decay of 4.0%), were corrected for decay, Lorentz and polarization effects, and empirical absorption corrections were based on the $\psi$-scan of four strong reflections (minimum and maximum transmission factors 0.613 and 1.000). Upon averaging the 5220 reflections, 4914 of which were uniquely measured, ($R_{int}=0.015$). 4161 reflections with $I>3\sigma(I)$ were considered observed and used in the structural analysis. The centric triclinic space group was confirmed by the successful refinement of the structure solved by heavy-atom Patterson methods and expanded using Fourier techniques[11] and refinement by full-matrix least squares using the MSC-Crystal Structure Package TEXSAN on a Silicon Graphics Indy computer.[12] Of the 47 non-H atoms, the 17 C atoms of the aliphatic chain from C(19) to C(35) have high thermal parameters and were refined isotropically, the other 30 atoms were refined anisotropically and the 47 H atoms at calculated positions with thermal parameters equal to 1.3 times that of the attached C atoms were not refined. Convergence for 339 variable parameters by least squares refinement on $F$ with $w=4\ F_o^2/\sigma^2(F_o^2)$, where $\sigma^2(F_o^2)=[\sigma^2(I)+(0.010\ F_o^2)^2]$ for 4161 reflections with $I>3\sigma(I)$ was reached at $R=0.036$ and $wR=0.038$ with a goodness-of-fit of 2.36. $(\Delta/\sigma)_{max}=0.03$. The final difference Fourier map was featureless, with maximum positive and negative peaks of 0.60 and 0.55 e $Å^{-3}$, respectively.

Full crystallographic details, excluding structure factors, have been deposited at the Cambridge Crystallographic Data Centre (CCDC). See Information for Authors, *J. Mater. Chem.*,

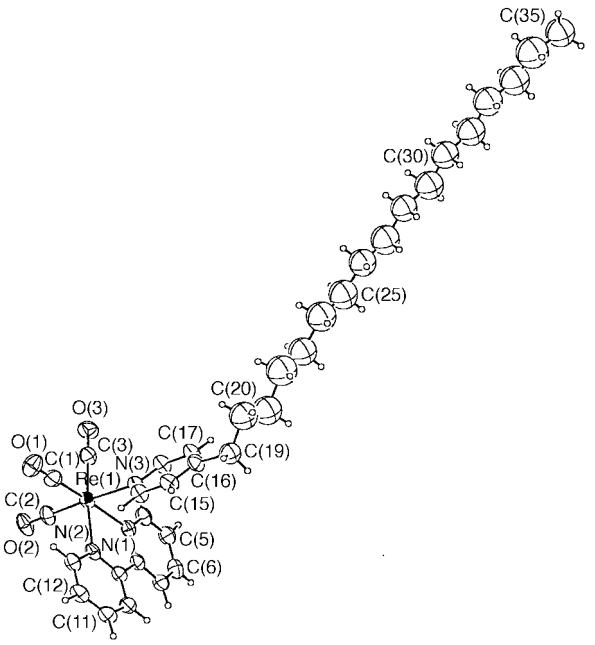


**Fig. 1** Perspective drawing of $[Re(CO)_3(bpy)\{py(CH_2)_{16}CH_3\}]^+$ with atomic numbering scheme. Thermal ellipsoids are shown at the 20% probability level.

1998, Issue 1. Any request to the CCDC for this material should quote the full literature citation and the reference number 1145/66.

## Results and Discussion

The $[Re(L)(CO)_3\{py(CH_2)_nCH_3\}]ClO_4$ complexes were synthesized by modification of a literature procedure reported for related rhenium(I) complexes.[6] All the newly synthesized complexes have been characterized by $^1H$ NMR, IR, positive-ion FABMS and gave satisfactory elemental analyses. All the complexes show an intense IR absorption band at *ca.* 1000–1100 $cm^{-1}$, typical of $\upsilon$(Cl–O) stretch for the perchlorate ion, and $\upsilon$(C–O) stretches at *ca.* 1900–2100 $cm^{-1}$, typical of the tricarbonyl rhenium(I) moiety in the facial arrangement. The X-ray crystal structure of $[Re(bpy)(CO)_3(pyC_{17}H_{35})]ClO_4$ has been determined.

### X-Ray crystallographic study

The perspective drawing of the cation of $[Re(bpy)(CO)_3(pyC_{17}H_{35})]^+$ is depicted in Fig. 1. The bond distances and angles are listed in Table 1.

The co-ordination geometry at the Re atom is distorted octahedral with the three carbonyl ligands arranged in a facial fashion. At the Re center, the *trans* angles subtended by $Re^I$ and the two co-ordinated atoms *trans* to each other are in the range of 172.6(3)–176.3(3)°, showing a slight deviation from an ideal octahedral arrangement. The rhenium–nitrogen bond lengths are typical of rhenium(I) diimine systems [2.160(6)–2.165(6) Å], with the slight differences being attributable to small differences in the π-back bonding. The Re—C—O bond angles of 176.4(7)–178.3(8)° are slightly distorted from linearity. The bond angle for N(1)—Re(1)—N(2) [74.8(2)°] is considerably smaller than 90°, as required by the bite distance exerted by the steric environment of the chelating bpy ligand. The Re(1)—C(2) bond length of 1.899(9) Å, which is *trans* to the pyridyl-surfactant ligand, is similar to those for the Re(1)—C(I) [1.90(1) Å] and Re(1)—C(3) [1.907(9) Å] bonds. Similar observations have been reported in other related rhenium(I) systems.[6h,i,13,14] The hydrophobic aliphatic chain on the pyridine unit is basically made up of a zigzag backbone of hydrocarbon, with the molecular arrangement resembling that of other long-chain molecules. It is interesting to note that the long aliphatic hydrocarbon chains between two neighboring cations are arranged in a head-to-tail fashion as shown in Fig. 2

**Table 1** Selected bond distances (Å) and angles (degrees) for $[Re(CO)_3(bpy)\{py(CH_2)_{16}CH_3\}]ClO_4$

| | | | |
|---|---|---|---|
| Re(1)—C(1) | 1.90(1) | Re(1)—C(2) | 1.899(9) |
| Re(1)—C(3) | 1.907(9) | Re(1)—N(1) | 2.160(6) |
| Re(1)—N(2) | 2.165(6) | Re(1)—N(3) | 2.209(6) |
| C(1)—O(1) | 1.164(10) | C(2)—O(2) | 1.153(8) |
| C(3)—O(3) | 1.154(8) | | |
| N(1)—Re(1)—C(1) | 172.6(3) | N(2)—Re(1)—C(3) | 172.9(3) |
| N(3)—Re(1)—C(2) | 176.3(3) | Re(1)—C(1)—O(1) | 177.7(9) |
| Re(1)—C(2)—O(2) | 176.4(7) | Re(1)—C(3)—O(3) | 178.3(8) |
| N(1)—Re(1)—N(2) | 74.8(2) | N(1)—Re(1)—N(3) | 83.7(2) |
| N(2)—Re(1)—N(3) | 84.5(2) | | |

### Electronic absorption spectroscopy

The electronic absorption spectra of complexes **1–14** in dichloromethane and aqueous 60 mM SDS (sodium dodecylsulfate) solution at room temperature all showed an absorption band at *ca.* 330–400 nm. With reference to previous spectroscopic work on rhenium(I) diimine systems,[6,14] this absorption band is assigned as the $d_\pi(Re)\rightarrow\pi^*$(bpy/phen) metal-to-ligand charge transfer (MLCT) transition (Table 2). In the case of the $Re^I$–bpy system, the MLCT absorption appeared as a characteristic band, while for the $Re^I$–phen complexes, the lowest MLCT absorption only appeared as a shoulder, and hence its absorption maximum could not be determined accurately.

A systematic study of the effect of solvent on the MLCT absorption energy was performed. For complex **6**, the $d_\pi(Re)\rightarrow\pi^*$(bpy) MLCT absorption band was found to red shift with reducing solvent polarity, *i.e.* from 351 nm (MeOH–$H_2O$ 7:3 v/v) to 360 nm ($CH_2Cl_2$). With reference to the pioneering work on solvatochromism of rhenium(I) tricarbonyl diimine halide complexes by Wrighton and co-workers,[6a–e] the Re—L (where L = diimine) bond distance would be distorted in the excited state. It was proposed that a shorter Re—L distance would be expected in the excited state. Although a lengthened Re—L bond would also accord well with the solvent effects, a shorter Re—L bond would be consistent with the notion that there would be an electrostatic attraction between the negatively charged L and the oxidized

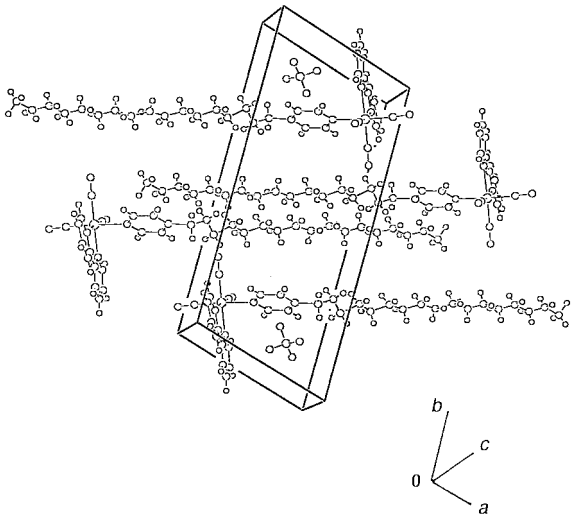


**Fig. 2** Perspective drawing of $[Re(CO)_3(bpy)\{py(CH_2)_{16}CH_3\}]ClO_4$ in the unit cell, showing that the long aliphatic hydrocarbons between two neighboring cations are arranged in a head-to-tail fashion

**Table 2** Photophysical data for $[Re(L)(CO)_3\{py(CH_2)_nCH_3\}]ClO_4$ complexes (**1–12**) and $[Re(L)(CO)_3\{4\text{-}PyCO(Chol)\}]ClO_4$ (**13–14**) at 298 K; L = bipy for **1–6, 13**; L = phen for **7–12, 14**

| complex | *n* | solvent | absorption $\lambda_{max}$/nm ($\varepsilon$/dm$^3$ mol$^{-1}$ cm$^{-1}$) | emission $\lambda_{em}$/nm ($\tau_o$/μs) |
|---|---|---|---|---|
| **1** | 0 | $CH_2Cl_2$ | 262 (18 400), 280(sh) (18 100), 308 (13 150), 322 (13 125), 360 (4250) | 550 (0.58) |
| | | MeOH | 252 (19 020), 264 (18 585), 308 (11 375), 320 (11 970), 355 (3780) | 563 (0.20) |
| | | MeOH–$H_2O$ (7 : 3 v/v) | 252 (18 775), 266 (18 100), 306 (11 615), 320 (12 500), 351 (3930) | 565 (0.20) |
| | | 60 mM SDS | 252 (19 250), 262 (19 005), 308 (11 240), 320 (11 450), 351 (3280) | 570 (0.15) |
| **2** | 1 | $CH_2Cl_2$ | 262 (18 525), 280(sh) (18 090), 308 (13 145), 322 (13 135), 360 (4350) | 550 (0.58) |
| | | 60 mM SDS | 252 (19 510), 262 (19 355), 308 (11 380), 320 (11 735), 351 (3620) | 570 (0.15) |
| **3** | 4 | $CH_2Cl_2$ | 262 (19 000), 280(sh) (18 500), 308 (13 390), 322 (13 280), 360 (4340) | 550 (0.58) |
| | | 60 mM SDS | 250 (14 290), 268 (13 850), 310 (9770), 322 (10 270), 350 (3120) | 570 (0.15) |
| **4** | 14 | $CH_2Cl_2$ | 264 (18 500), 282sh (17 850), 308 (13 625), 322 (12 940), 360 (4340) | 550 (0.58) |
| | | 60 mM SDS | 250 (12 850), 266 (12 300), 310 (9065), 322 (9450), 350 (3120) | 570 (0.15) |
| | | solid | — | 520 (1.5) |
| | | LB film | *ca.* 370(sh) | 526 |
| **5** | 16 | $CH_2Cl_2$ | 264 (17 520), 282(sh) (16 790), 308 (12 305), 322 (12 180), 360 (3980) | 550 (0.58) |
| | | 60 mM SDS | 250 (12 970), 266 (12 455), 310 (9265), 322 (9650), 350 (3600) | 570 (0.15) |
| | | solid | — | 520 (1.49) |
| | | LB film | *ca.* 370(sh) | 527 |
| **6** | 18 | $CH_2Cl_2$ | 264 (19 380), 282(sh) (18 170), 308 (13 140), 322 (12 760), 360 (4095) | 550 (0.58) |
| | | octanol | 310 (9300), 322 (9875), 354 (3730) | 555 (0.27) |
| | | hexanol | 310 (9355), 322 (9945), 354 (3860) | 560 (0.23) |
| | | MeOH | 252 (19 180), 264 (18 970), 306 (11 615), 320 (11 910), 352 (4090) | 563 (0.19) |
| | | MeOH–$H_2O$ (7 : 3 v/v) | 218(sh) (24 870), 250 (19 130), 268 (18 680), 308 (11 435), 320 (12 005), 351 (3720) | 565 (0.20) |
| | | MeCN | 218(sh) (19 330), 252 (17 760), 264 (18 580), 308 (12 760), 320 (13 720), 348 (4500) | 565 (0.22) |
| | | 60 mM SDS | 250 (12 260), 264 (11 965), 310 (8295), 320 (8565), 356 (3135) | 570 (0.15) |
| | | solid | — | 520 (1.39) |
| | | LB film | *ca.* 370(sh) | 526 |
| **7** | 0 | $CH_2Cl_2$ | 278 (26 680), 298(sh) (13 125), 336(sh) (4610), 370(sh) (3820), 395(sh) (2780) | 540 (3.3) |
| | | MeOH | 258 (19 245), 274 (21 580), 296(sh) (11 580), 327(sh) (5130), 365(sh) (3595), 395(sh) (2200) | 550 (1.2) |
| | | 60 mM SDS | 256 (30 570), 356 (36 920), 330(sh) (6825), 370(sh) (4780) 392(sh) (3350) | 565 (1.0) |
| **8** | 4 | $CH_2Cl_2$ | 276 (20 685), 326(sh) (4110), 378(sh) (3080) | 540 (3.3) |
| | | MeOH | 258 (20 245), 274 (22 580), 296(sh) (12 595), 327(sh) (5970), 365(sh) (3960), 395(sh) (2360) | 550 (1.2) |
| | | 60 mM SDS | 256 (23 830), 276 (30 265), 330(sh) (5850), 370(sh) (3940), 392(sh) (2690) | 565 (1.0) |
| **9** | 12 | $CH_2Cl_2$ | 278 (21 535), 296(sh) (11 270), 326(sh) (4050), 378(sh) (3230) | 540 (3.3) |
| | | MeOH | 258 (18 220), 276 (21 605), 294(sh) (11 405), 327(sh) (4580), 365(sh) (3020), 395(sh) (1490) | 550 (1.2) |
| | | 60 mM SDS | 256 (22 470), 276 (29 765), 330(sh) (6280), 370(sh) (3940), 392(sh) (2655) | 565 (1.0) |
| **10** | 14 | $CH_2Cl_2$ | 256 (21 670), 276 (28 665), 332(sh) (6170), 378(sh) (4785), 392(sh) (3985) | 540 (3.4) |
| | | MeOH | 258 (20 190), 273 (23 945), 292(sh) (13 400), 327(sh) (4570), 365(sh) (2990), 395(sh) (1510) | 550 (1.3) |
| | | 60 mM SDS | 298 (6640), 332(sh) (3280), 358(sh) (2220), 390(sh) (1555) | 565 (1.0) |
| | | solid | — | 518 (2.1) |
| | | LB film | *ca.* 330(sh) | 525 |
| **11** | 16 | $CH_2Cl_2$ | 262 (24 450), 278 (26 855), 334(sh) (4875), 374(sh) (3920), 396(sh) (2950) | 540 (3.2) |
| | | MeOH | 258 (18 215), 276 (21 615), 294(sh) (11 305), 327(sh) (4395), 365(sh) (2950), 395(sh) (1520) | 550 (1.1) |
| | | 60 mM SDS | 300 (6740), 332 (4245), 362(sh) (2855) | 565 (1.1) |
| | | solid | — | 518 (2.05) |
| | | LB film | *ca.* 330 (sh) | 525 |
| **12** | 18 | $CH_2Cl_2$ | 278 (21 395), 296(sh) (12 000), 336(sh) (5275), 370(sh) (4360), 395(sh) (3235) | 540 (3.3) |
| | | MeOH | 258 (23 615), 276 (27 880), 294(sh) (14 610), 327(sh) (5320), 365(sh) (3730), 395(sh) (2240) | 550 (1.2) |
| | | 60 mM SDS | 250 (37 045), 276 (65 285), 302(sh) (30 680), 329(sh) (5970), 370(sh) (3760) | 565 (1.0) |
| | | solid | — | 518 (2.05) |
| | | LB film | *ca.* 330(sh) | 525 |
| **13** | — | $CH_2Cl_2$ | 280 (18 490), 312 (15 575), 322 (16 235), 352 (6690) | 540 (0.83) |
| | | 60 mM SDS | 246 (16 860), 270 (15 130), 312 (14 280), 322 (16 385), 340 (8265) | 550 (0.26) |
| | | solid | — | 518 (1.48) |
| | | LB film | *ca.* 370(sh) | 528 |
| **14** | — | $CH_2Cl_2$ | 280 (21 400), 332 (9810), 384(sh) (3980) | 540 (3.6) |
| | | 60 mM SDS | 224(sh) (11 610), 260(sh) (6105), 276 (10 135), 328(sh) (7615), 474(sh) (6280) | 530 (2.2) |
| | | solid | — | 518 (2.0) |
| | | LB film | 340(sh), 390(sh) | 527 |

central metal. The contracted Re—L bond would also be consistent with the substitution inertness of the Re—L bond in the excited state. The contracted Re—L bond interpretation has been preferred since $d^5$ rhenium(II) complexes of nitrogen donors are generally more substitution inert than the $d^6$ rhenium(I) analogues. The ligating atom here is a nitrogen atom and there may well be a stronger bond between the formally $d^5$ $Re^{II}$ and any nitrogen donor ligand on the basis of 'hard' and 'soft' arguments. Thus for excited states with charge separation [*i.e.* $Re^{I}$–diimine→$Re^{II}$–diimine(−1)], solvents of different polarity would stabilize the charge separated state to different extent. For example, polar solvents would be expected to stabilize the charge separated state better than non-polar solvents. Since in polar media the ionic character of the charge separated excited state would be more preferentially stabilized, leading to a better charge separation, and hence a stronger electrostatic attraction between the $Re^{II}$ and the diimine(−1) center, and a greater Re—L bond contraction

resulted.[15] Recently, Sullivan reported on a detailed calculation of solvatochromism in organometallic systems,[15b] in which he suggested that the origin of the large solvatochromism observed in organometallic systems could be traced to the interaction of ground- and excited-state charge distributions with the solvent functioning as a dielectric medium. Solvatochromism of this magnitude was suggested to be due to a large dipole moment change upon excitation that was confined to a small effective molecular geometry, which in turn was a direct consequence of spatially non-demanding ligands like CO.

Besides studying the solvatochromism of the complexes, a systematic study of the effect of chain length variation on the absorption properties of the rhenium(I) surfactant complexes has been undertaken. According to the system studied by Demas and co-workers[16] on a series of related rhenium(I) diimine surfactant nitrile complexes, $[Re(CO)_3(bpy)\{CH_3(CH_2)_nCN\}]^+$ ($n=0$, 2, 5, 6, 7, 9, 10, 13, 17), the lowest energy absorption maximum was observed to blue-shift by at least 2500 $cm^{-1}$ with increasing $n$.[16] This observation has been suggested to arise from the folding of the long alkyl chain back to the diimine ring which lowered the local polarity.[17] As the diimine ring played an important role in the lowest energy absorption band which was tentatively assigned as a $d_\pi(Re)\rightarrow\pi^*$(diimine) MLCT transition, such a gradual change in the local polarity of the diimine environment as one increased the length of the chain $n$ would cause a significant shift of these charge transfer absorption bands, similar to that observed in solvatochromism.[15] In our present system unlike those reported by Demas and co-workers,[16] an increase in the length of the alkyl chain on the 4-alkylpyridine ligand did not cause a shift in the absorption band. It is suggested that either the fold-back mechanism of the long alkyl chain did not occur in the present system, or the long alkyl chain when it folded back did so to surround the pyridine ring rather than onto the diimine ring. As the pyridine ring was not directly involved in the lowest energy MLCT transition, no significant effect on the lowest energy absorption band would be observed.

### Emission spectroscopy

Excitation of the surfactant complexes **1–12** at $\lambda\geqslant350$ nm in fluid solution at room temperature resulted in intense yellowish green emission at *ca.* 530–580 nm of relatively long emissive lifetime. The photophysical data are summarized in Table 2. Given the relatively long excited-state lifetime and the large Stokes shift, it is likely that the emission is derived from states arising from a MLCT triplet excited state, similar to other related systems.[6,13–16] Solvatochromism has also been observed in the emission spectral data. For complex **6**, it was found that the more polar the solvent employed was, the lower would be the MLCT emission energy, *i.e.* 550 nm ($CH_2Cl_2$) *cf.* 565 nm (MeOH–$H_2O$ 7 : 3 v/v). The observation could be rationalized by arguments similar to that described for the solvatochromism observed in the electronic absorption spectra.

Similar to the absorption study, a systematic investigation of the effect of chain length variation on the photophysical properties of the rhenium(I) surfactant complexes has been undertaken. Unlike the related rhenium(I) surfactant nitrile system studied by Demas and co-workers,[16] where a variation in the alkyl chain length of the $NC(CH_2)_nCH_3$ ligand resulted in a dramatic perturbation of the excited state properties, almost no difference in the excited state properties was observed in our present system upon varying the alkyl chain length on the pyridyl ligand. In the surfactant nitrile system reported by Demas and co-workers,[16] the changes in the excited state properties that accompanied the change in the alkyl chain length in $H_2O$ were attributed to an intramolecular fold-back of the alkyl chain onto the face of the bipyridine ligand which changed the local solvent environment for the MLCT excited state.[16,17] This fold-back mechanism was further substantiated by addition of $\beta$-cyclodextrin to an aqueous solution of the rhenium(I) diimine surfactant nitrile complexes. In the absence of oxygen, the emission lifetime of the complexes was found to decrease with increasing [$\beta$-CD], suggesting the removal of the alkyl group from the bpy, exposing it to the surrounding aqueous medium or to the OH groups of the CD molecule. In either case enhanced deactivation of the excited state would occur, and the emission lifetime would shorten.[16] However, in our pyridyl surfactant system, the non-polar alkyl chain even if it did fold-back in polar solvents such as MeOH–$H_2O$ (7 : 3 v/v), it would do so by wrapping around the pyridine rather than the bipyridine unit. Since the pyridine unit is not directly involved in the MLCT excited state, it is not surprising to see that the MLCT excited state properties were not affected by the alkyl chain length to any considerable extent.

Besides the long-chain surfactant complexes, a cholesterolate containing pyridyl ligand, 4-pyridylcholesterolate [4-pyCO(Chol)] has also been synthesized and incorporated into the rhenium(I) system. Owing to the rigidity of the cholesterol backbone, no folding-back of the hydrophobic chain would be possible. Complexes **13** and **14** have been found to emit at similar wavelengths as complexes **1–12**. This further supports the fact that the long chain attached to the pyridine ligand in **1–12** does not affect the emission properties of the rhenium(I) diimine system to any significant extent.

### Photochemical properties

The phosphorescent state of the rhenium(I) tricarbonyl diimine complexes was found to be quenched by a variety of electron acceptors and donors. Pyridinium acceptors such as methyl viologen or 4-cyano-*N*-methylpyridinium ions were found to quench the phosphorescence with a $k_q$ value of *ca.* $10^8$ $dm^3$ $mol^{-1}s^{-1}$. On the other hand, electron donors such as TMPD were found to quench the phosphorescence more efficiently. The bimolecular quenching rate constants are summarized in Table 3. The bimolecular quenching rate constants appeared to depend on the reduction potential of the quenchers, suggestive of an electron transfer mechanism.

In order to establish the electron transfer nature of the quenching reactions of $[Re(CO)_3(bpy)\{py(CH_2)_nCH_3\}]^+$, transient absorption spectroscopic studies on **6** with methyl viologen ($MV^{2+}$) and diphenylamine (DPA) were performed. In the case of $MV^{2+}$ quenching, the spectrum was dominated by two bands, one at *ca.* 390 nm and the other broad band at *ca.* 600 nm; both of which are characteristic of the reduced methyl viologen cation radical and comparable to the literature reported spectrum.[18] The reaction mechanism is likely to involve an electron transfer step.

$$[Re(CO)_3(bpy)\{py(CH_2)_{18}CH_3\}]^{+}* + MV^{2+} \rightarrow [Re(CO)_3(bpy)\{py(CH_2)_{18}CH_3\}]^{2+} + MV^{\cdot+}$$

No additional bands due to the oxidized $[Re(CO)_3(bpy)\{py(CH_2)_{18}CH_3\}]^{2+}$ could be detected in these difference spectra. It is likely that the strong absorption of $MV^{\cdot+}$ has obscured the transient absorption of $[Re(CO)_3(bpy)\{py(CH_2)_{18}CH_3\}]^{2+}$.

Similarly, with DPA two characteristic transient absorption bands centered at *ca.* 400 and 680 nm were observed, which were characteristic of the absorption of the diphenylamine cation radical.[19] An electron transfer mechanism was established.

$$[Re(CO)_3(bpy)\{py(CH_2)_{18}CH_3\}]^{+}* + DPA \rightarrow [Re(CO)_3(bpy)\{py(CH_2)_{18}CH_3\}] + DPA^{\cdot+}$$

Similar to the oxidative quenching by $MV^{2+}$, no transient absorption bands due to the $[Re(CO)_3(bpy)\{py(CH_2)_{18}CH_3\}]$

**Table 3** Bimolecular quenching rate constants for $[Re(CO)_3(bpy)\{py(CH_2)_{18}CH_3\}]^+$ in degassed acetonitrile at 298 K

| quencher | $E(A^{0/-})$ or $E(D^{+/0})^a$/V | $k_q$/dm$^3$ mol$^{-1}$ s$^{-1}$ |
|---|---|---|
| methyl viologen[b] | −0.45 | $6.0\times10^8$ |
| 4-cyano-*N*-methylpyridinium[b] | −0.67 | $4.5\times10^8$ |
| TMPD | +0.34 | $1.1\times10^{10}$ |
| TMB | +0.43 | $3.7\times10^9$ |
| DPA | +1.07 | $5.1\times10^9$ |
| TPA | +1.10 | $5.6\times10^9$ |
| 1,4-dimethoxybenzene | +1.34 | $6.9\times10^8$ |
| 1,2,3-trimethoxybenzene | +1.42 | $1.5\times10^7$ |

[a]*vs.* SSCE, taken from ref. 25 and 26. [b]All the pyridinium salts are hexafluorophosphates.

transient species were observed, as the absorption coefficient of $DPA^{\cdot+}$ was far much larger than those of the reduced rhenium species. The transient signals in both cases were found to decay by second order kinetics, attributed to the back electron transfer reactions.

### Electrochemical properties

Cyclic voltammetric data for complexes **1–14** are collected in Table 4. Each complex showed a characteristic quasi-reversible oxidation wave, tentatively assigned as the oxidation of the metal center, *i.e.* $Re^{I}\rightarrow Re^{II}$, similar to that reported for related systems.[6,13b,14,20,21] For the reduction wave, the 2,2′-bipyridyl complexes showed two reduction waves, the first occurring at *ca.* −1.12 to −1.18 V, while the second is at *ca.* −1.38 to −1.41 V *vs.* SCE. The two reduction waves were tentatively assigned as the two successive one-electron reduction of 2,2′-bipyridine ligand and were comparable to the literature reported value on similar systems.[13b,14,20,21] For the 1,10-phenanthroline systems, only one reduction wave was observed, in the range of −1.12 to −1.14 V *vs.* SCE, and was assigned as the reduction of the 1,10-phenanthroline ligand.[13b,14,20,21] It is interesting to note that both the metal-centered oxidation and the diimine ligand-centered reduction did not seem to have significant dependence on the chain length of the surfactant pyridyl ligand. This lack of correlation between the reduction potential with the nature of the pyridyl ligand, either long aliphatic chain or cholesterolate ligand, suggested that the nature of the pyridine ligands has minimal effect, both electronic and steric, on the MLCT state.[14,20]

**Table 4** Electrochemical data for complexes **1–14**

| complex | $E_{1/2}$(red)[a,b]/V ($\Delta E$/mV) | $E_{1/2}$(ox)[a,c]/V ($\Delta E$/mV) |
|---|---|---|
| **1** | −1.12 (50), −1.38 (120) | +1.73 (42) |
| **2** | −1.18 (68), −1.42 (184) | +1.76 (86) |
| **3** | −1.16 (64), −1.40 (184) | +1.79 (150) |
| **4** | −1.15 (60), −1.36 (140) | +1.77 (130) |
| **5** | −1.18 (62), −1.38 (132) | +1.76 (136) |
| **6** | −1.18 (56), −1.41 (199) | +1.77 (130) |
| **7** | −1.13 (90) | +1.75 (76) |
| **8** | −1.14 (102) | +1.72 (88) |
| **9** | −1.13 (100) | +1.74 (84) |
| **10** | −1.13 (104) | +1.73 (86) |
| **11** | −1.13 (98) | +1.74 (88) |
| **12** | −1.12 (90) | +1.73 (72) |
| **13** | −1.15 (60), −1.38 (180) | +1.78 (130) |
| **14** | −1.15 (95) | +1.73 (88) |

[a]All the electrochemical measurements were performed in MeCN (0.1 mol dm$^{-3}$ $Bu^n_4NPF_6$). $E_{1/2}=(E_{pa}+E_{pc})/2$; $E_{pa}$=anodic peak potential; $E_{pc}$=cathodic peak potential; working electrode, glassy carbon; scan rate, 100 mV s$^{-1}$. $\Delta E=|E_{pa}-E_{pc}|$. [b]For 2,2′-bipyridine, the first reduction wave is reversible, while the second wave is found to be dependent on scan rate and is quasi-reversible; for 1,10-phenanthroline, the reduction wave is found to depend on scan rate, and is quasi-reversible. [c]All the oxidation waves were found to depend on scan rate, and are quasi-reversible.

### *π–A* Isotherms of the rhenium complexes

Selected *π–A* isotherms for the complexes are shown in Fig. 3. All curves showed one well defined condensed region with surface pressures >30 mN m$^{-1}$. In addition, the molecular areas (Å$^2$) obtained by the extrapolation of the condensed region to zero surface pressure were almost identical (for bpy systems *ca.* 110 Å$^2$ and for phen systems *ca.* 100 Å$^2$), and were larger than the calculated values (55 Å$^2$) based on the crystal structure of a model complex, $[Re(CO)_3(bpy)\{py(CH_2)_{16}CH_3\}]ClO_4$, which indicated a relatively loose packing of the complex in LB film with respect to the crystal state. The compression–expansion cycles of the *π–A* isotherms for the complexes showed hardly any observable hysteresis, indicative of the excellent film-forming properties of the complexes on the pure water subphase.

On the other hand, the molecular areas for the rhenium(I) complexes of the cholesterol type pyridyl ligand were found to be smaller than those of the corresponding long alkyl chain pyridyl ligand, *i.e.* for **6** the area is 110 Å$^2$ while for **13** it is 90 Å$^2$. Similarly, for the phen systems, **12** (100 Å$^2$) has an area larger than that of **14** (78 Å$^2$). It is likely that the cholesterol type pyridyl ligand, though more rigid than the long alkyl chain pyridyl ligand, has a better match with the bulky complex residue, such that the cholesterol complexes can orient themselves in a more ordered and closely packed form.

### Electronic absorption properties of the LB films

The electronic absorption data for the surfactant rhenium(I) diimine complexes in different environments, *i.e.* $CH_2Cl_2$, 60 mM SDS solution and LB films are summarized in Table 2. In addition, the absorbance shows a linear relationship to the number of layers deposited on the quartz plate for **6**, **13** and

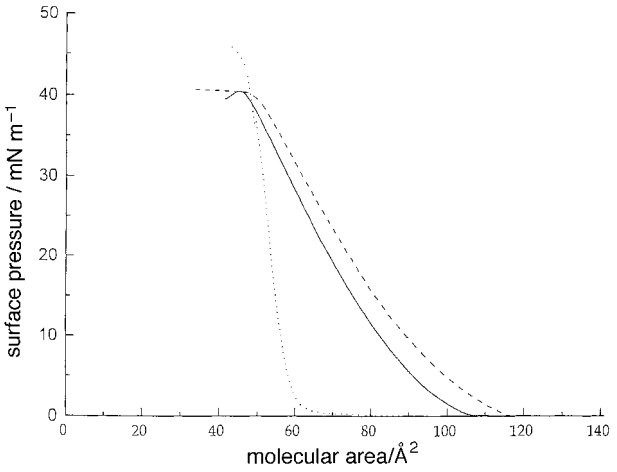


**Fig. 3** *π–A* isotherms of $[Re(CO)_3(bpy)\{py(CH_2)_{18}CH_3\}]^+$ (—), $[Re(CO)_3(phen)\{py(CH_2)_{18}CH_3\}]^+$ (– – –) and $[Re(CO)_3(phen)\{pyCO(Chol)\}]^+$ (……) on pure water

**14**. The electronic absorption spectra of **6** as a function of layer number are shown in Fig. 4.

The electronic absorption spectra showed a characteristic absorption band at *ca.* 370 nm for the bpy complexes (**4–6** and **13**), while bands at *ca.* 330 and 390 nm were observed for the phen complexes (**10–12** and **14**). Similar to the related rhenium(I) diimine systems,[6,14] these absorption bands are likely to be assigned as **MLCT** transition, *i.e.* $d_\pi(Re)\rightarrow\pi^*$(bpy/phen). Due to the very weak absorbance of the LB films, a very precise location of the absorption band was found to be impossible. It is interesting to note that the absorption bands of the complexes deposited on the LB films are red-shifted with respect to those in solution. For example, for the bpy systems, the absorption band which occurred at 360 nm in $CH_2Cl_2$ and 356 nm in 60 mM SDS, occurred at *ca.* 370 nm in LB films. It is suggested that rigidochromism is responsible for the observation. The increase in the rigidity of the environment would cause the lowering of the electronic absorption energies. For the aggregation studies, there is no significant change in the electronic absorption energy with respect to the LB films formed at various surface pressures.

In addition, it is interesting to note that the UV–VIS absorption spectra of the complexes in LB films did not show any significant change for storages of more than one month, indicative of the stability of the films formed.

### Emission properties of the LB films

The emission data of the complexes in different media are collected in Table 2. From the emission data, a characteristic yellowish green emission centered at *ca.* 525 nm for the complexes deposited on the quartz plate was observed. This emission is characteristic of rhenium(I) diimine systems and is assigned as the $^3$MLCT emission derived from the $d_\pi(Re)\rightarrow\pi^*$(bpy/phen) transition.[6,14]

The emission energies of the films and SDS solutions were found to be significantly blue shifted with respect to their solution states. For example, for the bpy systems, the emission occurred at *ca.* 550 nm in $CH_2Cl_2$ and 570 nm in 60 mM SDS solution, while in LB films it occurred at *ca.* 520 nm. Similar observations have also been found in the phen systems. The blue shift in emission energies of the complexes in LB films has also been attributed to the increasing rigidity of the environment relative to that in the solution state.[15]

For the aggregation studies on $[Re(CO)_3(bpy)\{py(CH_2)_{18}CH_3\}]ClO_4$, similar to the electronic absorption spectroscopy, the emission and excitation spectra showed no significant difference for the LB films deposited at various surface pressures.

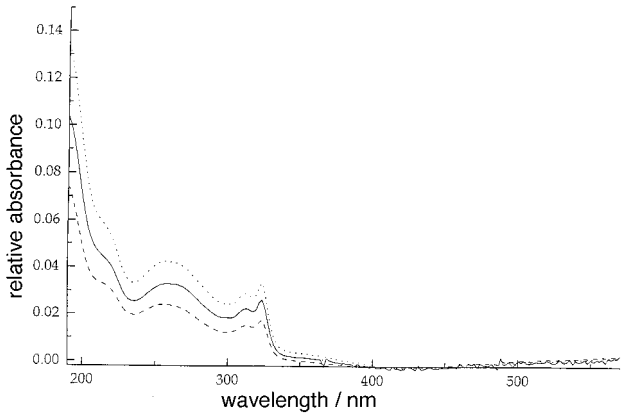


**Fig. 4** UV–VIS spectral traces of one (– – –), three (—) and five layers (……) of $[Re(CO)_3(bpy)\{py(CH_2)_{18}CH_3\}]^+$ deposited on a quartz plate by the LB technique

### Non-linear optical properties of the LB films

Owing to the similarity in the compositions and structures of the rhenium(I) surfactant complexes we have synthesized, we have chosen complex **6** as a representative sample for SHG measurements in LB films. The temporal profile of the SHG signal from the monolayer film of **6** is shown in Fig. 5. Although the signals were weak, they were appreciably different from that of the film-free blank substrate.

Given the equation

$$I_{2\omega} \propto (\chi^{(2)}(\theta) l\ I_\omega)^2/(n_\omega{}^2 n_{2\omega}) \quad (1)$$

in which $n_\omega$ and $n_{2\omega}$ are the refractive indices at 1064 and 532 nm, respectively, $l$ is the film thickness, $\chi^{(2)}(\theta)$ is the measured susceptibility uncorrected for angular dependence, $I_\omega$ is the fundamental frequency intensity, the second-order molecular hyperpolarizability $\beta$ is related to the non-linear optical susceptibility $\chi^{(2)}$ by:[22b]

$$\chi^{(2)} = N f_{2\omega}(f_\omega)^2 \beta \quad (2)$$

in which $f_{\omega,2\omega} = [(n_{\omega,2\omega})^2 + 2]/3$ is a local field correction factor, with $n_{2\omega}$ usually slightly larger than $n_\omega$. In the actual treatment, $n_\omega$ and $n_{2\omega}$ are taken to be 1.5. $N = 1/lA$ is the number of molecules per unit volume where $A$ is the molecular area of the film-forming materials under study.[22]

By using the ratio (*ca.* 1/30) of $I_{2\omega}(p\rightarrow p)$ for the monolayer film of **6** to that of the standard film made of (*E*)-*N*-methyl-4-[2-(4-octadecyloxyphenyl)ethenyl]pyridinium iodide (**BI**) ($\chi^{(2)} = 5.1\times10^{-7}$ esu, $\beta = 1.5\times10^{-28}$ esu), eqn. (1) and (2), as well as values of $A$ of 0.4 nm$^2$ for **BI** and 1.0 nm$^2$ for **6** and values of $l$ of 2.7 nm for **BI** and 2.5 nm for **6**, one can estimate $\chi^{(2)}$ to be $8.6\times10^{-8}$ esu and a $\beta$ value of $7.6\times10^{-29}$ esu for **6**. This $\beta$ value is comparable to that for 2-methyl-4-nitroaniline ($4.5\times10^{-29}$ esu).[23] Second harmonic generation from the LB film of a ruthenium(II) surfactant bipyridine derivative compound was first observed in 1989 and was attributed to a $d_\pi(Ru)\rightarrow\pi^*$(bpy) metal-to-ligand charge transfer (MLCT) transition,[24] with the transition dipole moment mainly oriented along the 2,2′-bipyridine moiety attached to the long alkyl chain. A similar mechanism of SHG in the ruthenium(II) complexes[24] may also operate in the present amphiphilic rhenium complexes studied, and the second-order molecular hyperpolarizability ($\beta$) may be dominated by the component along the pyridine moiety attached to the long alkyl chain. The second-order molecular hyperpolarizability ($\beta$) of the ruthenium(II) complex was estimated to be $7\times10^{-29}$ esu,[24] which was, however, derived from a 72-layer alternate LB film on each side of the substrate that showed a SH signal comparable to a reference film of known value {[1-methyl-4-(*N*-octadecyl-*N*-methylamino)styryl]pyridinium iodide, $\beta = 5\times10^{-28}$ esu}. It is of note that $\beta$ values could only be reasonably deduced from monolayer film but not multilayer film, and the film must only be on one side of the supported substrate and not on both sides of the substrate.

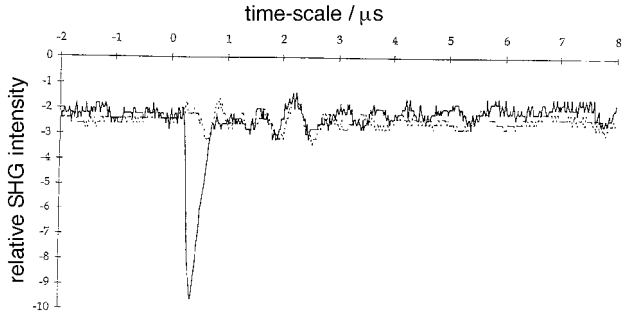


**Fig. 5** Plot of the SHG intensity *vs.* time (μs) for a blank quartz substrate (– – –) and a monolayer of $[Re(CO)_3(bpy)\{py(CH_2)_{18}CH_3\}]^+$ deposited on a quartz plate (—)

An independent solution state SHG measurement[27] on **6** using the method of Rayleigh hyperscattering gave a $\beta$ value of $9.5 \times 10^{-29}$ esu, comparable to that found in monolayer films.

V. W.-W. Y. acknowledges financial support from the Research Grants Council and The University of Hong Kong. V. C.-Y. L. acknowledges the receipt of a Croucher Foundation Scholarship, administered by the Croucher Foundation and a Sir Edward Youde Memorial Fund Fellowship, administered by the Sir Edward Youde Memorial Fund Council.

## References

1 (*a*) J. H. Fendler and E. J. Fendler, *Catalysis in Micellar and Macromolecular Systems*, Academic Press, New York, 1975; (*b*) R. D. Vold and M. J. Vold, *Colloid and Interface Chemistry*, Plenum Press, New York, 1986; (*c*) M. Grätzel, *Heterogeneous Photochemical Electron Transfer*, CRC Press, Boca Raton, FL, 1989; (*d*) *Photochemistry in Organized and Constrained Media*, ed. V. Ramamurthy, VCH, New York, 1991; (*e*) *Kinetics and Catalysis in Microheterogeneous Systems*, ed. M. Grätzel and K. Kalyanasundaram, Marcel Dekker, New York, 1991; (*f*) J.-H. Fuhrhop and J. Köning, *Membranes and Molecular Assemblies: The Synkinetic Approach*, The Royal Society of Chemistry, Cambridge, 1994.

2 (*a*) D. G. Whitten, C. Chesta, X. Ci, M. A. Kellett and V. W. W. Yam, *Photochemical Processes in Organized Molecular Systems*, ed. K. Honda, Elsevier, New York, 1991, p. 213; (*b*) D. G. Whitten, *Acc. Chem. Res*., 1980, **13**, 83; (*c*) D. G. Whitten, *Angew. Chem., Int. Ed. Engl*., 1979, **18**, 440; (*d*) D. G. Whitten, *Acc. Chem. Res*., 1980, **13**, 83; (*e*) D. G. Whitten, J. C. Russell and R. H. Schmehl, *Tetrahedron*, 1982, **38**, 2455; (*f*) J. H. Fendler, *J. Phys. Chem*., 1983, **89**, 2730; (*g*) M. H. Gehlen and F. C. De Schryver, *Chem. Rev*., 1993, **93**, 199.

3 (*a*) K. Kalyanasundaram, *Photochemistry of Polypyridine and Porphyrin Complexes*, Academic Press, London, 1992; (*b*) O. Horváth and K. L. Stevenson, *Charge Transfer Photochemistry of Coordination Compounds*, VCH, New York, 1993; (*c*) K. Kalyanasundaram, *Photochemistry in Microheterogeneous Systems*, Academic Press, New York, 1987; (*d*) *Energy Resources through Photochemistry and Catalysis*, ed. M. Grätzel, Academic Press, New York, 1983; (*e*) V. Balzani and F. Scandola, *Supramolecular Photochemistry*, Ellis Horwood, Chichester, 1991.

4 (*a*) G. Sprintschnik, H. W. Sprintschnik, P. P. Kirsch and D. G. Whitten., *J. Am. Chem. Soc*., 1976, **98**, 2337; (*b*) G. Sprintschnik, H. W. Sprintschnik, P. P. Kirsch and D. G. Whitten., *J. Am. Chem. Soc*., 1977, **99**, 4947; (*c*) R. H. Schmehl, L. G. Whiteside and D. G. Whitten, *J. Am. Chem. Soc*., 1981, **103**, 3761.

5 (*a*) V. W. W. Yam, V. C. Y. Lau and K. K. Cheung, *J. Chem. Soc., Chem. Commun*., 1995, 259; (*b*) V. W. W. Yam, V. C. Y. Lau and K. K. Cheung, *Organometallics*, 1995, **14**, 2749; (*c*) V. W. W. Yam, V. C. Y. Lau and K. K. Cheung, *Organometallics*, 1996, **15**, 1740; (*d*) V. W. W. Yam, K. K. Tam, M. C. Cheng, S. M. Peng and Y. Wang, *J. Chem. Soc., Dalton. Trans*., 1992, 1717; (*e*) V. W. W. Yam, K. K. Tam and T. F. Lai, *J. Chem. Soc., Dalton Trans*., 1993, 651; (*f*) V. W. W. Yam and K. K. Tam., *J. Chem. Soc., Dalton Trans*., 1994, 391; (*g*) V. W. W. Yam, K. K. Tam and K. K. Cheung, *J. Chem. Soc., Dalton Trans*., 1995, 2779; (*h*) V. W. W. Yam, K. K. W. Lo, K. K. Cheung and R. Y. C. Kong, *J. Chem. Soc., Chem. Commun*., 1995, 1191; (*i*) V. W. W. Yam, K. M. C. Wong, V. W. M. Lee, K. K. W. Lo and K. K. Cheung, *Organometallics*, 1995, **14**, 4034.

6 (*a*) M. S. Wrighton and D. L. Morse, *J. Am. Chem. Soc*., 1974, **96**, 998; (*b*) M. S. Wrighton, D. L. Morse and L. Pdungsap, *J. Am. Chem. Soc*., 1975, **97**, 2073; (*c*) P. J. Giordano, S. M. Fredericks, M. S. Wrighton and J. C. Luong, *J. Am. Chem. Soc*., 1978, **100**, 2257; (*c*) J. C. Luong, L. Nadjo and M. S. Wrighton, *J. Am. Chem. Soc*., 1978, **100**, 5790; (*d*); S. M. Fredericks, J. C. Luong and M. S. Wrighton, *J. Am. Chem. Soc*., 1979, **101**, 7415; (*e*) S. M. Fredericks and M. S. Wrighton, *J. Am. Chem. Soc*., 1980, **102**, 6166; (*f*) J. V. Caspar and T. J. Meyer, *J. Phys. Chem*., 1983, **87**, 952; (*g*) J. V. Caspar, B. P. Sullivan and T. J. Meyer, *Inorg. Chem*., 1984, **23**, 2104; (*h*) B. P. Sullivan, C. M. Bolinger, D. C. William, J. Vining and T. J Meyer, *J. Chem. Soc., Chem. Commun*., 1985, 1414; (*i*) P. Chen, R. Duesing, G. Tapolsky and T. J. Meyer, *J. Am. Chem. Soc*., 1989, **111**, 8305; (*j*) G. Tapolsky, R. Duesing and T. J. Meyer, *J. Phys. Chem*., 1989, **93**, 3885.

7 C. Osuch and R. Levine, *J. Am. Chem. Soc*., 1956, **78**, 1723.

8 F. E Ziegler and G. D. Berger, *Synth. Commun*., 1979, **9**, 539.

9 P. Martin and M. Szablewski, *Tensiometers and Langmuir-Blodgett Troughs, Operating Manual*, ed. F. Grunfield, Nima Technology, Coventry, 4th edn., 1989.

10 (*a*) S. K. Kurtz and T. T. Perry, *J. Appl. Phys*., 1968, **39**, 3798; (*b*) J. Jerphagnon and S. K. Kurtz, *J. Appl. Phys*., 1970, **41**, 1667.

11 PATTY: P. T. Beurskens, G. Admiraal, G. Beurskens, W. P. Bosman, S. Garica-Granda, R. O. Gould, J. M. M. Smits and C. Smykalla, The DIRDIF program system, Technical Report of the Crystallography Laboratory, University of Nijmegen, The Netherlands, 1992.

12 TeXsan: Crystal Structure Analysis Package, Molecular Structure Corporation, The Woodlands, TX, 1985 and 1992.

13 (*a*) E. Horn and M. R. Snow, *Aust. J. Chem*., 1980, **33**, 2369; (*b*) S. A. Moya, J. Guerrero, R. Pastene, R. Schmidt, R. Sariego, R. Sartori, J. Sanz-Aparicio, I. Fonseca and M. Martinez-Ripoll, *Inorg. Chem*., 1994, **33**, 2341; (*c*) J. C. Calabrese and W. Tam, *Chem. Phys. Lett*., 1987, **133**, 244.

14 (*a*) R. M. Leasure, L. Sacksteder, D. Nesselrodt, G. A. Reitz, J. N. Demas and B. A. DeGraff, *Inorg. Chem*., 1991, **31**, 3722; (*b*) A. P. Zipp, L. Sacksteder, J. Streich, A. Cook, J. N. Demas and B. A. DeGraff, *Inorg. Chem*., 1993, **32**, 5629; (*c*) L. Sacksteder, A. P. Zipp, E. A. Brown, J. Streich, J. N. Demas and B. A. DeGraff, *Inorg. Chem*., 1990, **29**, 4335; (*d*) L. Sacksteder, J. N. Demas and B. A. DeGraff, *Anal. Chem*., 1993, **65**, 3480; (*e*) J. R. Bacon and J. N. Demas, *Anal. Che*m., 1987, **59**, 2780; (*f*) E. R. Carraway, J. N. Demas and B. A. DeGraff, *Anal. Chem*., 1991, **63**, 337; (*g*) S. Boyde, G. F. Strouse, W. E. Jones, Jr. and T. J. Meyer, *J. Am. Chem. Soc*., 1989, **111**, 7448; (*h*) P. Chen, M. Curry and T. J. Meyer, *Inorg. Chem*., 1989, **28**, 2271; (*i*) G. Tapolsky, R. Duesing and T. J. Meyer, *Inorg. Chem*., 1990, **29**, 2285; (*j*) R. Duesing, G. Tapolsky and T. J. Meyer, *J. Am. Chem. Soc*., 1990, **112**, 5378; (*k*) P. Chen, R. Duesing, D. K. Graff and T. J. Meyer, *J. Phys. Chem*., 1991, **95**, 5850; (*l*) P. Chen, S. L. Mecklenburg and T. J. Meyer, *J. Phys. Chem*., 1993, **97**, 13126.

15 (*a*) R. N. Dominey, B. Hauser, J. Hubbard and J. Dunham, *Inorg. Chem*., 1991, **30**, 4754; (*b*) B. P. Sullivan, *J. Phys. Chem*., 1989, **93**, 24; (*c*) A. J. Lees, *Comments Inorg. Chem*., 1995, **17**, 319.

16 (*a*) G. A. Reitz, W. J. Dressick, J. N. Demas and B. A. DeGraff, *J. Am. Chem. Soc*., 1986, **108**, 5344; (*b*) G. A. Reitz, J. N. Demas, B. A. DeGraff and E. M. Stephens, *J. Am. Chem. Soc*., 1988, **110**, 5051.

17 (*a*) H. Sigel, *Angew, Chem., Int. Ed. Engl*., 1982, **21**, 389; (*b*) H. Sigel, B. E. Fischer and E. Farkas, *Inorg. Chem*., 1983, **22**, 925; (*c*) R. Malini-Balakrishnan, K. H. Scheller, U. K. Häring, R. Tribolet and H. Sigel, *Inorg. Chem*., 1985, **24**, 2067; (*d*) H. Sigel, R. Malini-Balakrishnan and U. K. Häring, *J. Am. Chem. Soc*., 1985, **107**, 5137.

18 T. Watanabe and K. Honda, *J. Phys. Chem*., 1982, **86**, 2617.

19 (*a*) T. Shida and W. H. Hamill, *J. Chem. Phys*., 1966, **44**, 2369; (*b*) T. Ohno and S. Kato, *Bull Chem. Soc., Jpn*., 1984, **57**, 1528.

20 (*a*) J. K. Hino, L. D. Ciana, W. J. Dressick and B. P. Sullivan, *Inorg. Chem*., 1992, **31**, 1072; (*b*) K. Kalyanasundaram, *J. Chem. Soc., Faraday Trans. 2*, 1986, **82**, 2401.

21 (*a*) S. A. Moya, R. Pastene, R. Schmidt, J. Cuerrero and R. Sartori, *Polyhedron*, 1992, **11**, 1665; (*b*) R. Lin, Y. Fu, C. P. Brock and T. F. Guarr, *Inorg. Chem*., 1992, **31**, 4336; (*c*) M. K. De Armond, K. W. Hanck and D. W. Wertz, *Coord. Chem. Rev*., 1985, **64**, 65; (*d*) J. B. Cooper, D. B. MacQueen, J. D. Petersen and D. W. Wertz, *Inorg. Chem*., 1990, **29**, 3701.

22 (*a*) G. J. Ashwell, R. C. Hargreaves and C. E. Baldwin, *Nature* (*London*), 1992, **357**, 5377; (*b*) D. Lupo, W. Prass, U. Scheunemann, A. Laschewsky, H. Ringsdorf and I. Ledoux, *J. Opt. Soc. Am. B*, 1988, *5*, 300; (*c*) T. G. Zhang, C. H. Zhang and G. K. Wang, *J. Opt. Soc. Am B*, 1990, **7**, 902; (*d*) Y. Q. Shen, J. F. Shen, L. Chiu, Z. Y. Zhu, X. F. Fu, Y. Xu, Y. Q. Liu, D. B. Zhu, W. C. Wang and L. Y. Liu, *Thin Solid Films*, 1992, **208**, 280.

23 C. C. Teng and A. F. Garito, *Phys. Rev. B*, 1983, **28**, 6766.

24 (*a*) H. Sakaguchi, H. Nakamura, T. Nakamura, T. Ogawa and T. Matsuo, *Chem. Lett*., 1989, 1715; (*b*) H. Sakaguchi, T. Nakamura and T. Matsuo, *Jpn. J. Appl. Phys*., 1991, **30**, L377; (*c*) H. Sakaguchi, T. Nakamura and T. Matsuo, *Appl. Organomet. Chem*., 1991, **5**, 257; (*d*) T. Matsuo, N. Nakamura, T. Nakao and M. Kawazu, *Chem. Lett*., 1992, 2363; (*e*) S. Yamada, T. Nakano and T. Matsuo, *Thin Solid Films*, 1994, **254**, 196.

25 J. L. Marshall, S. R. Stobart and H. B. Gray, *J. Am. Chem. Soc*., 1984, **106**, 3027.

26 G. J. Kavarnos and N. J. Turro, *Chem. Rev*., 1986, **86**, 401.

27 V. W. W. Yam, V. C. Y. Lau and C.-H. Huang, unpublished work.

*Paper* 7/05015A; *Received* 14*th July*, 1997